Theoretical and Applied Mechanics Letters 15 (2025) 100521

Contents lists available at ScienceDirect

Theoretical and Applied Mechanics Letters

journal homepage: www.elsevier.com/locate/taml

The significant contribution of stochastic forcing to nonlinear energy transfer in resolvent analysis

Youhua Wang[a,b], Ting Wu[b,*], Guowei He[b,c,*]

[a] Department of Modern Mechanics, University of Science and Technology of China, Hefei 230026, China
[b] The State Key Laboratory of Nonlinear Mechanics, Institute of Mechanics, Chinese Academy of Sciences, Beijing 100190, China
[c] School of Engineering Sciences, University of Chinese Academy of Sciences, Beijing 100049, China

ARTICLE INFO

Keywords:
Resolvent analysis
Energy transfer
Eddy viscosity
Stochastic forcing
Composite sweeping-enhanced resolvent

ABSTRACT

Nonlinear energy transfer is represented through eddy viscosity and stochastic forcing within the framework of resolvent analysis. Previous investigations estimate the contribution of eddy-viscosity-enhanced resolvent operator to nonlinear energy transfer. The present article estimates the contribution of stochastic forcing to nonlinear energy transfer and demonstrates that the contribution of stochastic forcing cannot be ignored. These results are achieved by numerically comparing the eddy-viscosity-enhanced resolvent operator and stochastic forcing with nonlinear energy transfer in turbulent channel flows. Furthermore, the numerical results indicate that composite resolvent operators can improve the prediction of nonlinear energy transfer.

Energy transfer plays a crucial role in turbulent flows, particularly in terms of nonlinear energy transfer. Energy transfer caused by the nonlinear term in the turbulent kinetic energy equation is referred to as nonlinear energy transfer. This transfer serves as the inter-scale transfer term in the spectral turbulent kinetic energy equation and plays a vital role in the energy distribution across scales. Numerous studies have explored the relationship between energy transfer, nonlinear energy transfer, turbulent dynamics, and coherent structures using the method such as spectral energy balance [1–9]. It is important to note that turbulence cannot be sustained by linear part alone; the inclusion of nonlinear effects, specifically nonlinear energy transfer, is indispensable.

However, incorporating the nonlinear term typically leads to substantial computational costs in numerical calculations. To address this issue, the resolvent method, based on linearized Navier-Stokes (N-S) equations, proposes treating the nonlinear term as input to the linearized system. This approach effectively reduces computational expenses and provides the space-time spectrum of velocity fluctuations as an output. As a necessary part of resolvent analysis, it is important to study the models of nonlinear forcing and the corresponding response. Researchers often employ stochastic forcing as input to the linear system to obtain statistical properties. The linearized N-S equations excited by white noise [10–16] have been widely used for this purpose. Stochastic forcing is referred to as nonlinear forcing that extracts energy from the mean field and transfers it to the fluctuating field. The nonlinear term in the N-S equations adheres to energy conservation principles. To account for dissipative effects, an eddy viscosity term is introduced, resulting in an enhanced resolvent method that includes both eddy viscosity and stochastic forcing.

By using nonlinear energy transfer, one can evaluate the models of nonlinear forcing in the resolvent method and in order to improve the prediction of the space-time spectrum. Symon et al. [9] compared the modes obtained from the resolvent analysis and the spatial proper orthogonal decomposition modes in direct numerical simulation (DNS). They found that the resolvent analysis accurately predicts the wave speed associated with the highest energy only at the scale with the highest growth rate. Through an analysis of transport induced by the eddy viscosity term, it is observed that derivatives of eddy viscosity result in a larger eddy viscosity transport.

It is important that nonlinear energy transfer in the eddy-viscosity-enhanced resolvent method should encompass not only the transport caused by eddy viscosity but also the influence of stochastic forcing. The combined effect of these two components constitutes a complete characterization of nonlinear energy transfer in the eddy-viscosity-enhanced resolvent method. The present article focuses on evaluating the nonlinear energy transfer in the eddy-viscosity-enhanced resolvent method and emphasizing the significance of stochastic forcing. This paper is organized as follows: firstly, we introduce the eddy-viscosity-enhanced resolvent and provide the calculation of nonlinear energy transfer in resolvent analysis. Subsequently, we present the results obtained from DNS and resolvent methods. Additionally, we calculate the results of the composite sweeping-enhanced resolvent method [17], which employs dynamic auto-regression to map white noise input to colored noise and

* Corresponding authors.
E-mail addresses: wuting@imech.ac.cn (T. Wu), hgw@lnm.imech.ac.cn (G. He).

https://doi.org/10.1016/j.taml.2024.100521
Received 31 January 2024; Received in revised form 26 March 2024; Accepted 29 March 2024
Available online 2 April 2024

introduces random sweeping into the resolvent method for turbulent shear flows.

Consider a turbulent channel flow, which is homogeneous in the streamwise and spanwise directions. In the subsequent descriptions, $\mathbf{u} = [u_1, u_2, u_3]^{\mathrm{T}} = [u, v, w]^{\mathrm{T}}$ represents the velocity fluctuation vector, x and z represent the streamwise and spanwise coordinates, while $y \in (-h, h)$ represents the wall-normal coordinate. The symbol $\hat{\cdot}$ represents spatial Fourier mode in (x, z), and $\tilde{\cdot}$ represents spatial-temporal Fourier mode in (x, z) and t. The variables k_x and k_z denote streamwise and spanwise wavenumbers, respectively, and $k^2 = k_x^2 + k_z^2$.

(1) The conventional resolvent can be briefly described as follows. The N-S equations can be expressed in the input-output form as:

$$\tilde{\mathbf{u}} = \mathbf{R}\tilde{\mathbf{F}}, \tag{1}$$

where $\tilde{\mathbf{F}}$ represents the nonlinear term in the N-S equations and is treated as the nonlinear forcing in the resolvent analysis. The linear parts of N-S equations are represented by the resolvent operator $\mathbf{R}$, which is given as

$$\mathbf{R} = \mathbf{B}^{\mathrm{T}}\left(-i\omega\begin{bmatrix}\mathbf{I} & \\ & 0\end{bmatrix} - \begin{bmatrix}\mathbf{L} & -\hat{\nabla} \\ -\hat{\nabla}^{\mathrm{T}} & 0\end{bmatrix}\right)^{-1}\mathbf{B}, \tag{2}$$

$$\mathbf{L} = \begin{bmatrix}-ik_xU + \nu\hat{\nabla}^2 & -U' & 0 \\ 0 & -ik_xU + \nu\hat{\nabla}^2 & 0 \\ 0 & 0 & -ik_xU + \nu\hat{\nabla}^2\end{bmatrix}, \tag{3}$$

$$\mathbf{B} = \begin{bmatrix}\mathbf{I} \\ 0\end{bmatrix}, \tag{4}$$

where $\mathbf{I}$ represents the identity matrix, $\hat{\nabla} = [ik_x, \partial_y, ik_z]^{\mathrm{T}}$. The variables ω and i represent the temporal frequency and the imaginary unit, respectively.

(2) In the eddy-viscosity-enhanced resolvent, the nonlinear forcing is modeled as:

$$\mathbf{F} = \nabla\cdot\left[\frac{1}{Re_\tau}\frac{\nu_{\mathrm{t}}}{\nu}\left(\nabla\mathbf{u} + \nabla\mathbf{u}^{\mathrm{T}}\right)\right] + \mathbf{f} = \mathbf{D}_{\nu_{\mathrm{t}}}\mathbf{u} + \mathbf{f}. \tag{5}$$

Here the stochastic forcing $\mathbf{f}$ is represented by spatial-temporal white noise, and eddy viscosity ν_{t} is used as the Cess model [18,19]; $\mathbf{D}_{\nu_{\mathrm{t}}}$ is given as

$$\mathbf{D}_{\nu_{\mathrm{t}}} = \frac{1}{Re_\tau\nu}\begin{bmatrix}\nu_{\mathrm{t}}\left(\partial_y^2 - k^2\right) + \nu_{\mathrm{t}}'\partial_y & ik_x\nu_{\mathrm{t}}' & 0 \\ 0 & \nu_{\mathrm{t}}\left(\partial_y^2 - k^2\right) + 2\nu_{\mathrm{t}}'\partial_y & 0 \\ 0 & ik_z\nu_{\mathrm{t}}' & \nu_{\mathrm{t}}\left(\partial_y^2 - k^2\right) + \nu_{\mathrm{t}}'\partial_y\end{bmatrix}. \tag{6}$$

Here $\nu_{\mathrm{t}}' = \mathrm{d}\nu_{\mathrm{t}}/\mathrm{d}y$.

By submitting Eq. (5) into Eq. (1), we obtain

$$\tilde{\mathbf{u}} = \mathbf{R}_{\nu_{\mathrm{t}}}\tilde{\mathbf{f}}. \tag{7}$$

It is noted that $\mathbf{R}_{\nu_{\mathrm{t}}}$ is the eddy-viscosity-enhanced resolvent, given by

$$\mathbf{R}_{\nu_{\mathrm{t}}} = \mathbf{B}^{\mathrm{T}}\left(-i\omega\begin{bmatrix}\mathbf{I} & \\ & 0\end{bmatrix} - \begin{bmatrix}\mathbf{L} + \mathbf{D}_{\nu_{\mathrm{t}}} & -\hat{\nabla} \\ -\hat{\nabla}^{\mathrm{T}} & 0\end{bmatrix}\right)^{-1}\mathbf{B}. \tag{8}$$

Due to the fact that nonlinear energy transfer is caused by nonlinear forcing, we can write the spatial Fourier mode of Eq. (5) in its components and multiply them by $\hat{u}_j^*$, the nonlinear energy transfer can be obtained:

$$\hat{N}_{\nu_{\mathrm{t}}} = \underbrace{\Re\left\{\frac{1}{Re_\tau\nu}\left(\nu_{\mathrm{t}}\langle\frac{\partial^2\hat{u}_j}{\partial\hat{x}_i^2}\hat{u}_j^*\rangle + \frac{\mathrm{d}\nu_{\mathrm{t}}}{\mathrm{d}y}\langle\left(\frac{\partial\hat{u}_j}{\partial\hat{z}} + \frac{\partial\hat{w}}{\partial\hat{x}_j}\right)\hat{u}_j^*\rangle\right)\right\}}_{\hat{T}_{\nu_{\mathrm{t}}}} + \underbrace{\Re\left\{\langle\hat{f}_j\hat{u}_j^*\rangle\right\}}_{\hat{T}_{\mathbf{f}}}, \tag{9}$$

where * represents the complex conjugation, $\Re$ represents the real part of the result. $\hat{T}_{\nu_{\mathrm{t}}}$ represents the contribution of the eddy viscosity transport, and $\hat{T}_{\mathbf{f}}$ represents the contribution of the stochastic forcing term. The eddy viscosity transport in Ref. [9] is the first term $\hat{T}_{\nu_{\mathrm{t}}}$ in Eq. (9).

Equation (9) can be written in the operator form as

$$\begin{aligned}\hat{N}_{\nu_{\mathrm{t}}} &= \Re\left\{\langle\mathrm{tr}\left(\hat{\mathbf{F}}\hat{\mathbf{u}}^*\right)\rangle\right\} \\ &= \Re\left\{\langle\mathrm{tr}\left[\left(\mathbf{D}_{\nu_{\mathrm{t}}}\hat{\mathbf{u}} + \hat{\mathbf{f}}\right)\hat{\mathbf{u}}^*\right]\rangle\right\} \\ &= \Re\left\{\langle\mathrm{tr}\left(\mathbf{D}_{\nu_{\mathrm{t}}}\hat{\mathbf{u}}\hat{\mathbf{u}}^* + \hat{\mathbf{f}}\hat{\mathbf{f}}^*\mathbf{R}_{\nu_{\mathrm{t}}}^*\right)\rangle\right\} \\ &= \Re\left\{\mathrm{tr}\left(\mathbf{D}_{\nu_{\mathrm{t}}}\mathbf{R}_{\nu_{\mathrm{t}}}\langle\hat{\mathbf{f}}\hat{\mathbf{f}}^*\rangle\mathbf{R}_{\nu_{\mathrm{t}}}^*\right) + \mathrm{tr}\left(\langle\hat{\mathbf{f}}\hat{\mathbf{f}}^*\rangle\mathbf{R}_{\nu_{\mathrm{t}}}^*\right)\right\},\end{aligned} \tag{10}$$

where tr represents the trace of a matrix. The cross-spectrum of stochastic forcing is given by

$$\left\langle\hat{\mathbf{f}}(k_x, k_z, y)\hat{\mathbf{f}}^*(k_x, k_z, y')\right\rangle = \mathbf{I}\delta\left(y - y'\right). \tag{11}$$

(3) In the composite sweeping-enhanced resolvent [17], the nonlinear forcing is determined by:

$$\hat{\mathbf{F}} = -\sqrt{k_x^2V_x^2(y) + k_z^2V_z^2(y)}\hat{\mathbf{u}} + \lambda_y\left(k_x, k_z, y\right)\partial_y\left(V_y(y)\partial_y\right)\hat{\mathbf{u}} + \hat{\mathbf{f}} = \mathbf{D}_{\mathrm{s}}\hat{\mathbf{u}} + \hat{\mathbf{f}}, \tag{12}$$

where $\mathbf{D}_{\mathrm{s}} = \mathrm{diag}\{D_{\mathrm{s}}, D_{\mathrm{s}}, D_{\mathrm{s}}\}$, and $D_{\mathrm{s}} = -\sqrt{k_x^2V_x^2(y) + k_z^2V_z^2(y)} + \lambda_y(k_x, k_z)\partial_y(V_y(y)\partial_y)$. The sweeping velocities $V_x(y) = \sqrt{\langle u^2(y)\rangle}$, $V_y(y) = \sqrt{\langle v^2(y)\rangle}$, $V_z(y) = \sqrt{\langle w^2(y)\rangle}$, and the characteristic length scale $\lambda_y\left(k_x, k_z, y\right) = \sqrt{V_y^2\left\langle\left|\partial_y\hat{\mathbf{u}}\right|^2\right\rangle/\left\langle\left|\partial_y\left(V_y(y)\partial_y\right)\hat{\mathbf{u}}\right|^2\right\rangle}$ are taken from DNS data.

The composite sweeping-enhanced resolvent can be expressed as

$$\tilde{\mathbf{u}} = \mathbf{R}_{\mathrm{s}}^2\tilde{\mathbf{f}}. \tag{13}$$

The sweeping-enhanced resolvent operator $\mathbf{R}_{\mathrm{s}}$ is defined by:

$$\mathbf{R}_{\mathrm{s}} = \mathbf{B}^{\mathrm{T}}\left(-i\omega\begin{bmatrix}\mathbf{I} & \\ & 0\end{bmatrix} - \begin{bmatrix}\mathbf{L} + \mathbf{D}_{\mathrm{s}} & -\hat{\nabla} \\ -\hat{\nabla}^{\mathrm{T}} & 0\end{bmatrix}\right)^{-1}\mathbf{B}. \tag{14}$$

The nonlinear energy transfer of the composite sweeping-enhanced resolvent can also be obtained by taking the components of Eq. (12) and multiply them by $\hat{u}_j^*$:

$$\hat{N}_{R_{\mathrm{s}}} = \Re\left\{D_{\mathrm{s}}\langle\hat{u}_j\hat{u}_j^*\rangle + \langle\hat{f}_j\hat{u}_j^*\rangle\right\}. \tag{15}$$

Equation (15) can be written in the operator form as

$$\hat{N}_{R_{\mathrm{s}}} = \Re\left\{\mathrm{tr}\left(\mathbf{D}_{\mathrm{s}}\mathbf{R}_{\mathrm{s}}^2\langle\hat{\mathbf{f}}\hat{\mathbf{f}}^*\rangle\mathbf{R}_{\mathrm{s}}^{*2} + \mathbf{R}_{\mathrm{s}}\langle\hat{\mathbf{f}}\hat{\mathbf{f}}^*\rangle\mathbf{R}_{\mathrm{s}}^{*2}\right)\right\} \tag{16}$$

where the cross-spectrum of stochastic forcing is given by

$$\left\langle\hat{\mathbf{f}}(k_x, k_z, y)\hat{\mathbf{f}}^*(k_x, k_z, y')\right\rangle = \mathbf{I}\left[k_x^2V_x^2(y) + k_z^2V_z^2(y)\right]^{3/2}\left\langle v^2(y)\right\rangle\delta\left(y - y'\right). \tag{17}$$

We utilized the DNS data of turbulent channel flow at $Re_\tau = 550$ in this work, which has been validated in our previous studies [17,20,21]. The nonlinear energy transfer of the DNS results is shown in Fig. 1(a) and (d), calculated in terms of the formula $\hat{N}\left(k_x, k_z; y\right) = -\left\langle\hat{u}_j^*\frac{\partial}{\partial\hat{x}_i}\left(\widehat{u_iu_j}\right)\right\rangle$.

Figure 1 (b) and (e) plot the nonlinear energy transfer $\hat{N}_{\nu_{\mathrm{t}}}$ of the eddy-viscosity-enhanced resolvent. The positive (colored in red) and negative (colored in blue) nonlinear energy transfer qualitatively consistent with the DNS results in terms of the distribution in streamwise (Fig. 1(b)) and spanwise (Fig. 1(e)) wavenumbers, respectively, and the wall-normal location. But the positive region is closer to the wall and the negative region is smaller than the DNS results.

Figure 1 (c) and (f) plot the energy transfer $\hat{T}_{\nu_{\mathrm{t}}}$ caused by eddy viscosity alone, without the inclusion of stochastic forcing. Notably, the areas and locations of negative and positive regions shows greater deviations from the DNS results, indicating that the nonlinear energy transfer of the eddy-viscosity-enhanced resolvent should encompass both the transport induced by eddy viscosity and the energy injection from stochastic forcing.

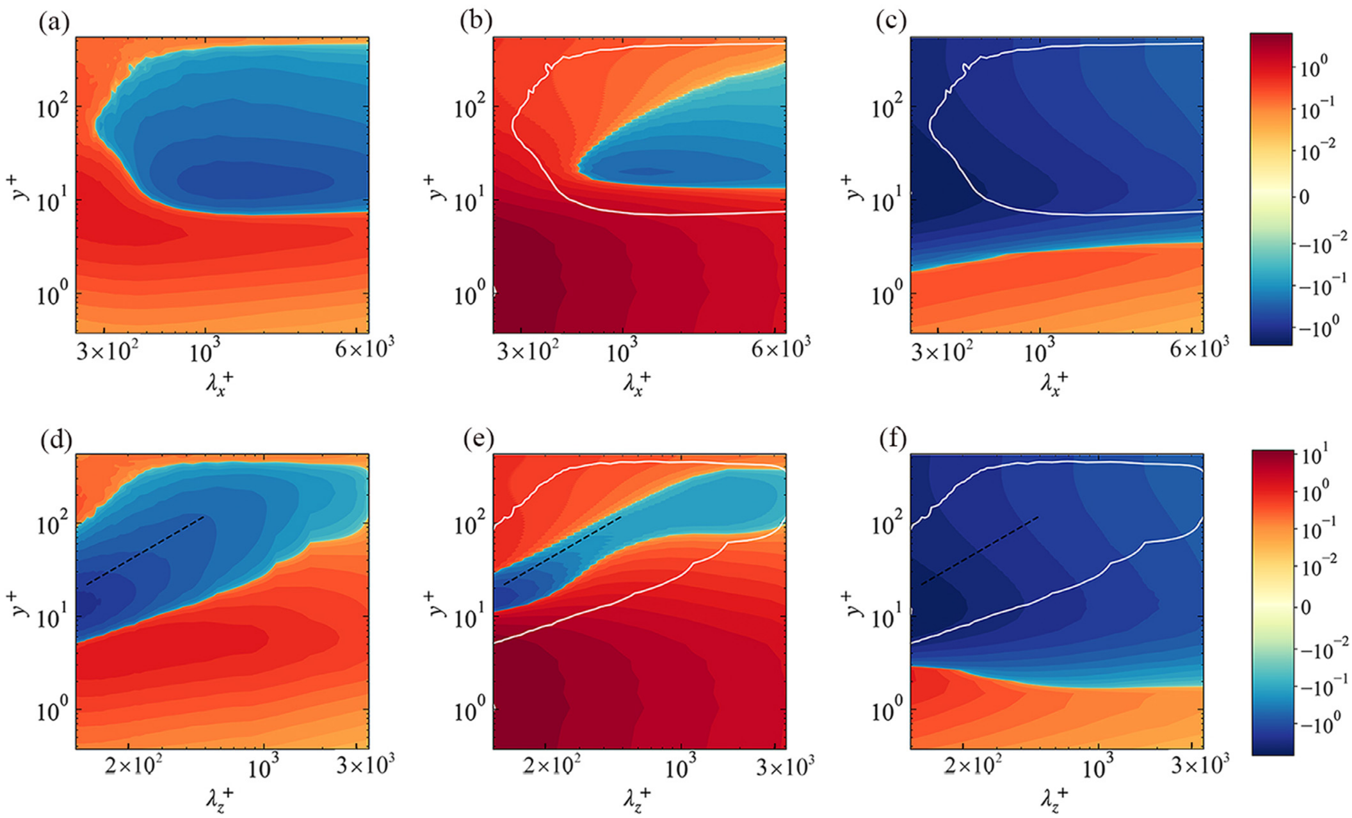

Fig. 1. One dimensional premultiplied spectrum of nonlinear energy transfer. (a) and (d), DNS results; (b) and (e), nonlinear energy transfer of eddy-viscosity-enhanced resolvent, $\hat{N}_{\nu_t} = \hat{T}_{\nu_t} + \hat{T}_{\mathbf{f}}$; (c) and (f), eddy viscosity transport of eddy-viscosity-enhanced resolvent, $\hat{T}_{\nu_t}$. The white solid line represents the contour corresponding to zero value of DNS results, the black dased line in spanwise premultiplied spectrum represent the variance of negative peak spanwise scale with wall-normal height.

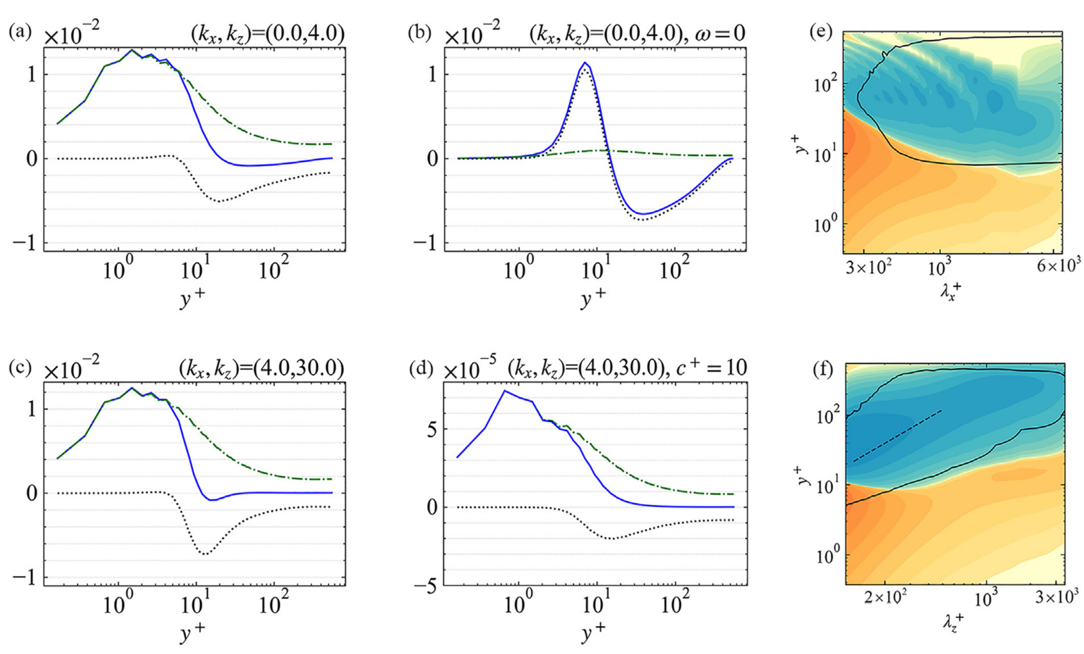

Fig. 2. (a)-(d), Wall-normal distribution of nonlinear energy transfer for eddy-viscosity-enhanced resolvent at specific wavenumbers. (a) and (c), Ensemble(time) averaged results; (b) and (d), at specific frequencies or wave speeds. Blue solid line, $\hat{N}_{\nu_t} = \hat{T}_{\nu_t} + \hat{T}_{\mathbf{f}}$; black dashed line, eddy viscosity transport $\hat{T}_{\nu_t}$; green dotted dashed line, stochastic forcing effect $\hat{T}_{\mathbf{f}}$. (e)-(f), One dimensional premultiplied spectrum of nonlinear energy transfer of the composite sweeping-enhanced resolvent. The color bars correspond to those in Fig. 1.

To illustrate the wall-normal distributions of the nonlinear energy transfer for the eddy-viscosity-enhanced resolvent, we considered specific wavenumbers and frequencies corresponding to the results of Symon et al. [9]. These results are presented in Fig. 2(a)-(d). We can obseve that in Fig. 2(a), (c) and (d), the black dashed line representing eddy viscosity transport is significantly different from the blue solid line representing the total nonlinear energy transfer. This indicates that although eddy viscosity transport at $(k_x, k_z) = (0, 4)$ with $\omega = 0$ yields effective outcomes in Fig. 2(b), the energy injection caused by stochastic forcing is significant for both the ensemble average and other frequency results.

In Fig. 2(e)-(f), we investigated the nonlinear energy transfer predicted by the composite sweeping-enhanced resolvent introduced in Ref. [17], calculated according to Eq. (15). The result exhibits a closer agreement in the areas and locations of positive and negative regions with the DNS results compared to the predictions of the eddy-viscosity-enhanced resolvent shown in Fig. 1. It indicates that the composite sweeping-enhanced has shown the effective improvements in predicting the nonlinear energy transfer.

In this paper, we conducted numerical analysis of nonlinear energy transfer in two models: the eddy-viscosity-enhanced resolvent and the composite sweeping-enhanced resolvent. The main results can be summarized as follows: (1) The nonlinear energy transfer of the eddy-viscosity-enhanced resolvent consists of two components: the transport induced by eddy viscosity and the energy injection from stochastic forcing. (2) The contribution of energy injection caused by stochastic forcing cannot be ignored in the eddy-viscosity-enhanced resolvent. (3) The composite sweeping-enhanced resolvent can improve the prediction of nonlinear energy transfer compared to the eddy-viscosity-enhanced resolvent. This study demonstrates the importance of stochastic forcing in resolvent analysis. The results obtained can be improved by use of the composite resolvents.

Declaration of competing interest

The authors declare that they have no known competing financial interests or personal relationships that could have appeared to influence the work reported in this paper.

CRediT authorship contribution statement

Youhua Wang: Conceptualization, Data curation, Formal analysis, Investigation, Software, Validation, Visualization, Writing – original draft. **Ting Wu:** Formal analysis, Investigation, Methodology, Project administration, Supervision, Validation, Writing – review & editing. **Guowei He:** Funding acquisition, Project administration, Supervision, Validation, Writing – review & editing.

Acknowledgments

This work was supported by the National Natural Science Foundation of China (NSFC) Basic Science Center Program for Multiscale Problems in Nonlinear Mechanics (Grant No. 11988102).

References

[1] I.A. Bolotnov, R.T. Lahey Jr, D.A. Drew, et al., Spectral analysis of turbulence based on the dns of a channel flow, Comput. Fluids 39 (4) (2010) 640–655.
[2] A. Cimarelli, E. De Angelis, C. Casciola, Paths of energy in turbulent channel flows, J. Fluid Mech. 715 (2013) 436–451.
[3] Y. Mizuno, Spectra of energy transport in turbulent channel flows for moderate reynolds numbers, J. Fluid Mech. 805 (2016) 171–187.
[4] M. Cho, Y. Hwang, H. Choi, Scale interactions and spectral energy transfer in turbulent channel flow, J. Fluid Mech. 854 (2018) 474–504.
[5] M. Lee, R.D. Moser, Spectral analysis of the budget equation in turbulent channel flows at high reynolds number, J. Fluid Mech. 860 (2019) 886–938.
[6] S. Symon, S.J. Illingworth, I. Marusic, Energy transfer in turbulent channel flows and implications for resolvent modelling, J. Fluid Mech. 911 (2021) A3.
[7] B. Jin, S. Symon, S.J. Illingworth, Energy transfer mechanisms and resolvent analysis in the cylinder wake, Phys. Rev. Fluid. 6 (2) (2021) 024702.
[8] H. Wang, Z. Yang, T. Wu, et al., Coherent structures associated with inter-scale energy transfer in turbulent channel flows, Phys. Rev. Fluid. 6 (10) (2021) 104601.
[9] S. Symon, A. Madhusudanan, S.J. Illingworth, et al., Use of eddy viscosity in resolvent analysis of turbulent channel flow, Phys. Rev. Fluid. 8 (6) (2023) 064601.
[10] B.F. Farrell, P.J. Ioannou, Stochastic forcing of the linearized navier-stokes equations, Phys. Fluid. A: Fluid Dyn. 5 (11) (1993) 2600–2609.
[11] B.F. Farrell, P.J. Ioannou, Perturbation structure and spectra in turbulent channel flow, Theor. Comput. Fluid Dyn. 11 (3-4) (1998) 237–250.
[12] B. Bamieh, M. Dahleh, Energy amplification in channel flows with stochastic excitation, Phys. Fluid. 13 (11) (2001) 3258–3269.
[13] M.R. Jovanović, B. Bamieh, Componentwise energy amplification in channel flows, J. Fluid Mech. 534 (2005) 145–183.
[14] O. Semeraro, V. Jaunet, P. Jordan, et al., Stochastic and harmonic optimal forcing in subsonic jets, 2016, In 22nd AIAA/CEAS Aeroacoustics Conference, Lyon, France, May 30-June 1. 2935
[15] O.T. Schmidt, A. Towne, G. Rigas, et al., Spectral analysis of jet turbulence, J. Fluid Mech. 855 (2018) 953–982.
[16] L. Lesshafft, O. Semeraro, V. Jaunet, et al., Resolvent-based modeling of coherent wave packets in a turbulent jet, Phys. Rev. Fluid. 4 (6) (2019) 063901.
[17] T. Wu, G. He, Composition of resolvents enhanced by random sweeping for large-scale structures in turbulent channel flows, J. Fluid Mech. 956 (2023) A31.
[18] R. Cess, A survey of the literature on heat transfer in turbulent tube flow, Res. Rep. (1958) 8–0529.
[19] W. Reynolds, A. Hussain, The mechanics of an organized wave in turbulent shear flow. Part 3. Theoretical models and comparisons with experiments, J. Fluid Mech. 54 (2) (1972) 263–288.
[20] T. Wu, C. Geng, Y. Yao, et al., Characteristics of space-time energy spectra in turbulent channel flows, Phys. Rev. Fluid. 2 (8) (2017) 084609.
[21] T. Wu, G. He, Stochastic dynamical model for space-time energy spectra in turbulent shear flows, Phys. Rev. Fluid. 6 (5) (2021) 054602.